Journal of Materials Chemistry A

Accepted Manuscript

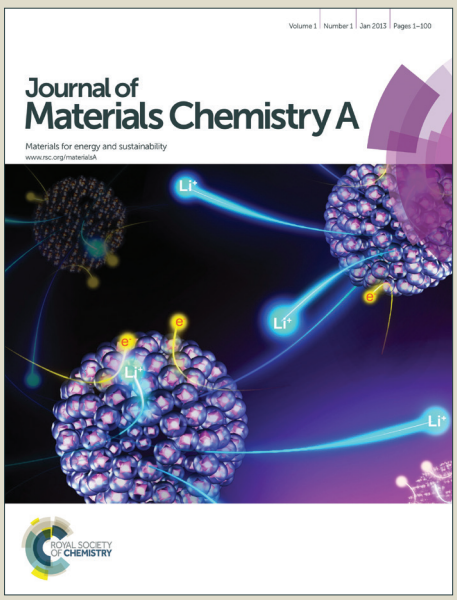

ROYAL SOCIETY OF CHEMISTRY

www.rsc.org/materialsA

Journal Name

RSCPublishing

ARTICLE

A new D-A-π-A type organic sensitizer based on substituted dihydroindolo [2, 3-b] carbazole and DPP unit with a bulky branched alkyl chain for highly efficient DSCs

Cite this: DOI: 10.1039/xoxxoooooox

Received ooth January 2012,
Accepted ooth January 2012

DOI: 10.1039/xoxxoooooox

www.rsc.org/

Guojian Tian,[a] Shengyun Cai,[a] Xin Li,[b] Hans Ågren,[b] Qiaochun Wang,[a] Jinhai Huang [a*] and Jianhua Su [a*]

Two new D-A-π-A configuration metal-free organic sensitizers (**T1**-**T2**) based on 5,7-dihexyl-6,12-diphenyl-5,7-dihydroindolo[2,3-b]carbazole and DPP unit with a bulky branched alkyl chain have been synthesized for dye-sensitized solar cells. Duo to a bulky branched alkyl chain has been attached to the donor and DPP unit, both compounds obtain high V_{oc} values. Under standard global AM 1.5 solar light condition, the **T1** based-device give a high conversion efficiency of 8.24 % with a J_{sc} of 15.72 mA cm^{-2}, a V_{oc} of 0.74 V and a *FF* of 0.71. These excellent performances make the donor dihydroindolo [2, 3-b] carbazole and DPP unit promising candidates for the further application in DSCs.

Introduction

Dye-sensitized solar cells (DSCs) are one of the most promising candidates for solving the impending energy problems due to their advantages of environmental friendliness, low material/fabrication cost and high conversion efficiencies.[1] Most organic dyes are composed of a donor-π-acceptor (D-π-A) configuration because of its effective photo-induced intramolecular charge transfer charateristic.[2] Recently, perovskite-based solar cells have drawn great attention in photovoltaic devices with their conversion efficiencies over 15 %.[3] However, the use of lead is a weakness, the widespread application of perovskite-based solar cells remains other environmentally friendly metals being explored. In DSCs, the organic sensitizers show molecular tailoring flexibility as a result of their D-π-A configuration and various π-conjugated bridges. The molecular structure exert an important effect on tuning the molecular energy gap, thus strongly affect the device performances.[4]

Diketopyrrolopyrroles (DPPs) have aroused great scientific interest in photochemical devices due to their exceptional photochemical, mechanical and thermal stabilities.[5] Recently, Tian and coworkers have put forward a new sensitizer structure, namely D-A-π-A configuration.[6] In view of the efficient intramolecular charge transfer and the appropriate electron-withdrawing properties, DPP moiety is suitable for fabricating the D-A-π-A configuration sensitizer, which can also be useful to distribute the electron and stabilize the sensitizer.[7] Thus, DPP is a favourable candidate for constructing highly efficient dyes in DSCs.

As is well known, short circuit photocurrent density (J_{sc}) and open circuit voltage (V_{oc}) should be taken into consideration in the design of dye, due to their importance to the overall conversion efficiency. In our previous study, we synthetized an excellent donor 5,7-dihexyl-6,12-diphenyl-5,7-dihydroindolo [2,3-b]carbazole with strong donating ability and well photo-stability.[8(a), (b)] However, the absorption spectra were not broad because of its unfavourable π-conjugated system, resulting in the short circuit current (J_{sc}) was not large. Considering the high V_{oc} value could be obtained by connecting long alkyl chains to the donor of sensitizer, these alkyl chains could reduce the π-π aggregation of the dyes and suppress the charge recombination.[9] In this work, we synthetized two new D-A-π-A sensitizers with 5,7-dihexyl-6,12-diphenyl-5,7-dihydroindolo[2,3-b]carbazole as the donor, thiophene and phenyl as the linker, DPP and cyanoacrylic acid as the acceptor.(Scheme 1) The molecular structure with bearing a bulky branched alkyl chain, the V_{oc} value will become higher, what's more, the donor with its powerful donating ability will further broaden the absorption spectrum and resulting in a larger J_{sc}, excellent performance of both two dyes could be anticipated.

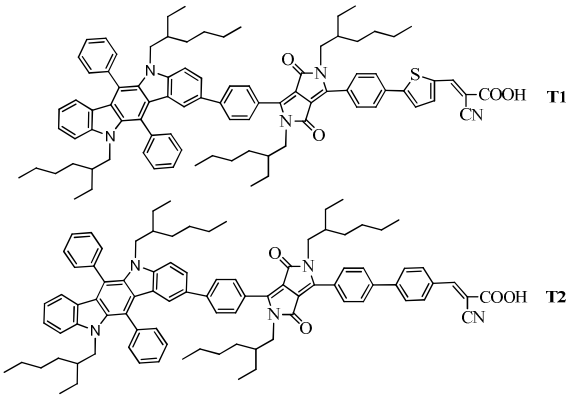

Scheme 1 Molecular structures of dyes (**T1**-**T2**).

Results and Discussion

Synthesis

The synthetic procedures of two dyes **T1-T2** were showed in Scheme 2. The donor moiety **D** was prepared according to the previous procedure, [8(a), (b)] as well as the **DPP** unit.[7] The two π-spacer **D2** and **D3** moieties were facilely commercial and without further purification. The Suzuki coupling of **D-Br** and **DPP** gave the intermediate **D-DPP**. Further Suzuki reaction of **D-DPP** with **D2** and **D3** yielded the aldehyde precursor **D-DPP-1** and **D-DPP-2**, respectively. The final products were obtained by the Knoevenagel condensation of aldehyde precursor and cyanoacetic acid. The purification of intermediates was performed by flash column chromatography and subsequent HPLC. All the intermediates and final products were characterized by standard spectroscopic methods including ^{1}H NMR, ^{13}C NMR and HRMS.

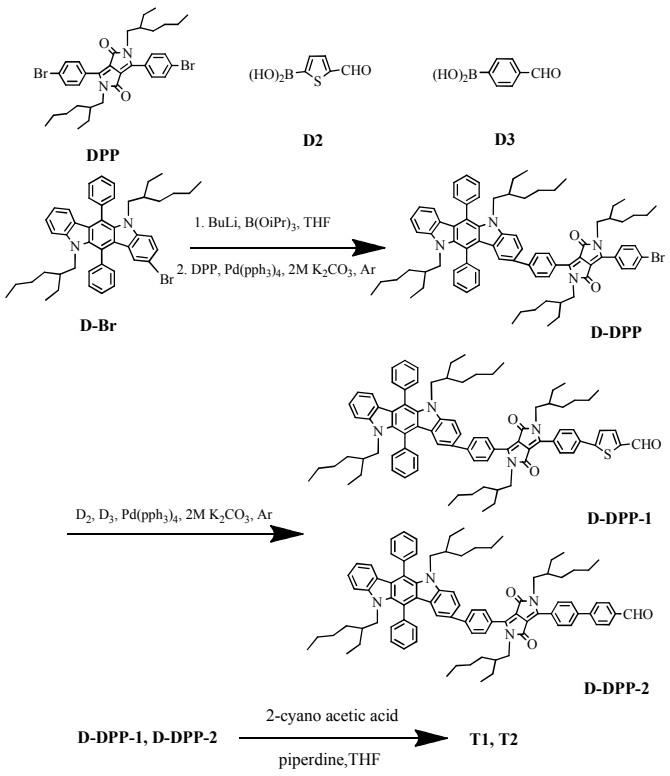

Scheme 2 Synthetic route to dyes **T1-T2.**

Optical properties

To figure up the light harvesting ability of these two dyes, UV/Vis absorption spectra were measured in a diluted solution of CH_2Cl_2 (1.0×10^{-5} M) and on TiO_2 films (3 μm thick). The data was listed in Table 1 and the spectra were showed in Fig. 1. In the visible light region, **T1** and **T2** both revealed two absorption bands: the major and broad absorption band were located at 450-650 nm with the maximum absorption at 521 nm and 508 nm, respectively, which was attributed to the charge transfer (CT) transition between the donor and the acceptor, the high intensity of these bands were well-correlated with the large value of oscillator strength (Table 1); the other narrower absorption band were located at 421 nm and 424 nm, respectively, which were ascribed to the localized aromatic π-π* transitions.[10] The absorption peak for the CT bands of **T1** showed red-shifted by 13 nm compared to that of **T2**, the corresponding maximum molar extinction coefficients at CT bands exhibited 3.05×10^4 and 3.13×10^4 M^{-1} cm^{-1}. The maximum molar extinction coefficients for the other absorption bands of **T1-T2** at 400-440 nm reached up 3.50×10^4 and 1.93×10^4 M^{-1} cm^{-1}, respectively. These high molar extinction coefficients indicated that both dyes had good light harvesting ability and a correspondingly thinner nanocrystalline film was allowed so as to avoid the decrease in the film's mechanical strength. This also benefited the electrolyte diffusion in the films and reduced the recombination possibility of the light induced charges during transportation.[11] As to the CT bands for both dyes, three points were noteworthy: 1) to be expected, the introduction of thiophene unit instead of benzene unit did surely result in red shifted absorption bands; 2) with the introduced DPP unit, both dyes exhibited slightly red shifted absorption bands than that of the previous dyes; 3) the dye with its donating group bearing a bulky alkyl chain displayed slightly lower values of the maximum molar extinction coefficients of the CT bands compared to the sensitizers reported previously.[8(a)]

The absorption spectra of **T1-T2** on thin transparent films (3 μm thick) after 12 h adsorption in CH_2Cl_2 solution were shown in Fig. 1. It was obvious that in 400-450 nm regions the absorption peak of **T1** on TiO_2 films were blue shifted by 39 nm compared to the solution, while **T2** exhibited slightly blue shifted by 2 nm. In 450-650 nm region, the absorption peak on TiO_2 films and in solution for **T1** were correspondingly blue shifted by 7 nm, but **T2** exhibited red shifted by 3 nm. These blue shifted and red shifted phenomena had been observed in many organic dyes on TiO_2 films.[12]

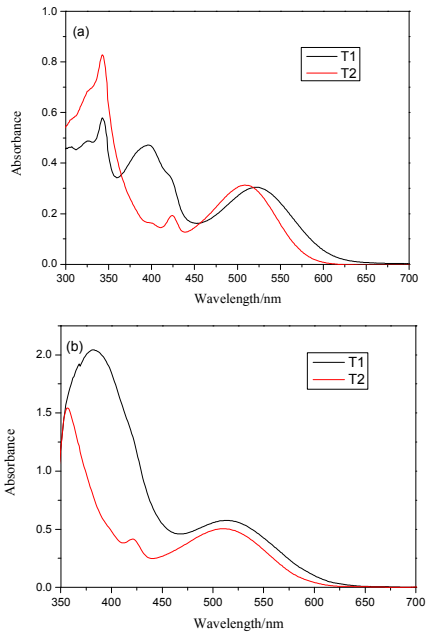

Fig. 1 (a) UV-Vis absorption spectra of **T1-T2** in CH_2Cl_2 (1.0×10^{-5} M); (b) absorption spectra of **T1-T2** adsorbed on TiO_2 films.

Electrochemical properties

The cyclic voltammogram of **T1-T2** were depicted in the Fig. 2, measured with two sensitizers attached on a 8 μm nanocrystalline TiO_2 films deposited on conducting FTO glass

■ **Table 1** Optical and electrochemical properties of **T1-T2**.

Dye	Calculated energy(eV, nm)	f^a	$\lambda_{max}{}^b$/nm (ε^g /10^4M^{-1}cm^{-1})	$\lambda_{max}{}^c$/nm on TiO_2	$E_{0\text{-}0}{}^d$	$E_{HOMO}{}^e$ (V)	$E_{LUMO}{}^f$ (V)
T1	2.46 , 503 [h]	1.64	396 (4.71), 421 (3.50), 521 (3.05)	382, 514	2.11	0.71	-1.40
T2	2.56 , 485	1.37	399 (1.64), 424 (1.93), 508 (3.13)	422, 511	2.18	0.72	-1.46

[a] Oscillator strengths at CT bands calculated by DFT/B3LYP; [b] Absorption maximum in CH_2Cl_2 solution; [c] Absorption maximum on TiO_2 films; [d] $E_{0\text{-}0}$: 0–0 transition energy measured at the intersection of absorption and emission spectra; [e] HOMOs were measured in CH_3CN containing 0.1 M $(n\text{-}C_4H_9)_4NPF_6$ with a scan rate of 100 mV s^{-1} (working electrode: Pt; reference electrode: SCE); calibrated with ferrocene/ferrocenium (Fc/Fc+) as an external reference. Counter electrode: Pt wire; [f] E_{LUMO} was calculated by $E_{ox} - E_{0\text{-}0}$; [g] Absorption coefficient; [h] Wavelength of the calculated oscillator strength *in vacuo*.

in CH_3CN containing 0.1 M $TBAPF_6$ as the supporting electrolyte with a 0.1 V s^{-1} scan rate and the results were listed in Table 1. In the Fig. 2, both dyes displayed two major semireversible waves: the lower one was derived from the oxidation of the donor, while the higher one could be ascribed to the oxidation of the DPP and π-spacer moieties.[13] The HOMO levels of **T1** (0.71 V *vs*. NHE) were almost similar with **T2** (0.72 V *vs.* NHE), and which were sufficiently positive compared to that of electrolyte pair I^-/I_3^- (ca. 0.40 V *vs*. NHE), thus ensured the smooth electron flow from the electrolyte to the dyes. The LUMO levels were calculated by the values of E_{ox} and the $E_{0\text{–}0}$ band gaps, which were estimated by the intersection of absorption and emission spectra. The LUMO levels of **T1** (-1.40 V *vs.* NHE) were also similar with **T2** (-1.46 V *vs.* NHE), which was also considerably negative compared to the conductive band level of TiO_2 (ca. -0.5 V *vs*. NHE). Therefore, electron injection of both dyes was guaranteed to be efficient.

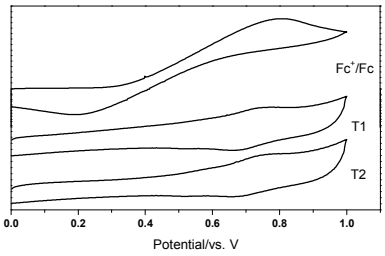

Fig. 2 The cyclic voltammogram of **T1-T2.**

Computational Analysis

To obtain further insight into the geometrical configuration and electron distribution of the frontier orbitals of the two dyes, the density functional theory (DFT) calculations were employed to optimize the ground state geometries of compounds **T1** and **T2** using the hybrid B3LYP functional[14] and the 6-31G* basis set.[15] At the optimized geometries, time-dependent (TD) DFT calculations were carried out to provide insight into molecular orbital compositions of the excited singlet states, using the range-separated CAM-B3LYP functional[16] and Ahlrichs's triple-ζ basis set def-TZVP.[17]All calculations were carried out using the Gaussian09 program package.[18]

DFT calculations suggest that the dihedral angles in compounds **T1** and **T2** (Fig. 3) were in general quite similar except that the dihedral angle δ exhibited a notable difference, due to the different steric effects of the thiophene and the phenyl rings. A more planar conformation of **T1** (smaller δ) was expected to enhance the π-conjugation of the molecule, leading to the fact that **T1** had an additional absorption band at around 400 nm compared with **T2**. This absorption band aroused from the electronic transition from HOMO-4 to LUMO (see Table 2 and 3) (ESI†), that was, the local excitation of the acceptor part of **T1**. The HOMO-4→LUMO transition of compound **T2** contributed negligibly to the absorption spectra. For both **T1** and **T2**, the first and fifth excited states contributed significantly to the absorption spectra (Fig. 4) (ESI†). These excited states correspond to transitions from HOMO-2 and HOMO-1 to LUMO and LUMO+1, i.e. successive electron transfer from the donor part to the acceptor part. In particular, compound **T1** offered larger oscillator strength at the absorption at around 500 nm and an additional absorption band at around 400 nm compared with **T2**, thus exhibiting higher photo-conversion efficiency.

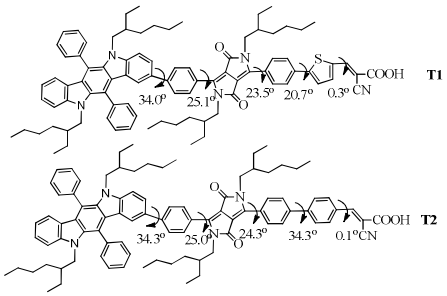

Fig. 3 Dihedral angles between the neighbouring units.

DSCs performance

The DSCs were fabricated based on the previous procedure to investigate the light harvesting ability of **T1-T2**.[8(a)] Fig. 5(a) exhibited the action spectra of incident photon-to-current conversion efficiency (IPCE) for DSCs with two dyes using the $CHCl_3$-EtOH (v/v 3:7) and CH_2Cl_2 as the soaking solvent. Particularly using the $CHCl_3$-EtOH (v/v 3:7) as the soaking solvent, both dyes based-device gave a strong and broad response in the visible light region, especially in the region from 360 nm to 610 nm with the IPCE exceeded 70%, and the highest value of 85.4% was obtained at 560 nm for **T1**, while a relatively response spectrum with the highest value of 79.7% at 540 nm for **T2**. The difference between the IPCE spectra of **T1** and **T2** was consistent with the difference of their absorption spectra as shown in Fig. 1. The higher IPCE values for **T1**

imply efficient charge transfer upon photo-excitation, partly due to the efficient electron communication.[19]

The photocurrent-voltage (*J-V*) plots of DSCs based on both dyes were showed in Fig. 5(b). The detailed parameters, i.e., short circuit current (J_{sc}), open circuit photovoltage (V_{oc}), fill factor (*FF*), and solar-to-electricity conversion efficiency (η) measured under AM 1.5 solar light (100 mW cm^{-2}) were listed in Table 4. The dyes soaked in mixed solvent $CHCl_3$-EtOH (v/v 3:7), the **T1** based-device gave a short circuit photocurrent density (J_{sc}) of 15.7 ± 0.20 mA cm^{-2}, an open circuit voltage (V_{oc}) of 739 ± 10 mV, and a fill factor (*FF*) of 0.71 ± 0.02, corresponding to an overall conversion efficiency (η), derived from the equation $\eta = J_{sc}V_{oc}FF$/light intensity, of 8.24%; while the **T2** based-device gave a J_{sc} of 14.85 ± 0.20 mA cm^{-2}, a V_{oc} of 765 ± 10 mV, a *FF* of 0.69 ± 0.02, and η of 7.83% under the same condition. These excellent performances were better than those reported dyes,[8(a), (b)] due to its bulky branched alkyl chain resulting in a high V_{oc} and the DPP unit facilitated its intramolecular charge transfer efficiently. The differences in the efficiency come mainly from the differences in their J_{sc}. The higher J_{sc} of **T1** was consistent with its higher and broader IPCE spectrum compared with that of **T2**. However, the dyes soaked in CH_2Cl_2, the efficiency (η) of both dyes become slightly low, under this condition. The reason why the dyes soaked in the mixed solvent $CHCl_3$-EtOH (v/v 3:7) behaved better than in CH_2Cl_2 was very complicated, including the diversified interactions among dyes, solvents, electrolytes and semiconductor surface, which could alter the optical and chemical properties of dyes and semiconductor.[20] Also, the solvent effect could pose an influence on the adsorbed amount of dyes on the TiO_2 films. The absorption amounts of **T1-T2** in $CHCl_3$: EtOH (*v*/*v* 3:7) and CH_2Cl_2 were showed in Table 5(ESI†).From the above, **T1** was a promising candidate for its excellent performance to be applied in DSCs.[21]

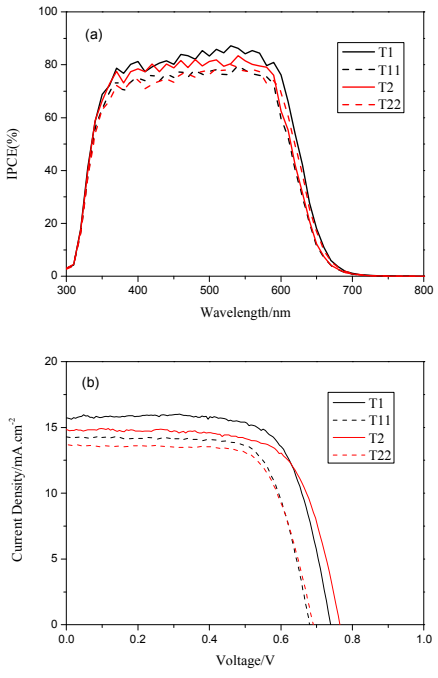

Fig. 5 The performances of DSCs sensitized by **T1-T2**: (a) IPCE spectra for DSCs based on **T1-T2** with dye baths in $CHCl_3$: EtOH (*v*/*v* 3:7) and CH_2Cl_2 (**T11-T22**); (b) I-V curves for DSCs based on **T1-T2** with dye baths in $CHCl_3$: EtOH (*v*/*v* 3:7) and CH_2Cl_2 (**T11-T22**) upon AM 1.5 solar light irradiation.

Table 4 The performances of DSCs based on **T1-T2**.

Dye	Solvents[a]	J_{sc}/mAcm^{-2}	V_{oc}/V	*FF* (%)	E_{ff}(%)
T1	CH_2Cl_2	14.28	0.680	72	6.95
T2	CH_2Cl_2	13.62	0.691	71	6.67
T1	$CHCl_3$- EtOH (*v*/*v* 3:7)	15.72	0.739	71	8.24
T2	$CHCl_3$- EtOH (*v*/*v* 3:7)	14.85	0.765	69	7.83

Electrochemical impedance spectroscopy

Electrochemical impedance spectroscopy (EIS) of the DSCs was carried out to further study the sensitizer's effect on the V_{oc} of the devices. The Nyquist plots of **T1-T2** based-device under a forward bias of 0.70V in the dark with a frequency range of 0.1 Hz to 100 kHz were shown in Fig. 6(a). The Bode plots were shown in Fig. 6(b). In Nyquist plots, two semicircles were observed, the left side was small and not conspicuous and it represented the redox charge-transfer response at the Pt/electrolyte interface, while the large semicircle could be ascribed to the electron-transfer impedance at the TiO_2/dye/electrolyte interface. In general, it was related to the charge recombination rate, and a smaller R_{rec} indicated a faster charge recombination. The radius of the bigger semicircle R_{rec} values decreased in the order of **T2** > **T1**, and the results were obvious consistent with the order of V_{oc} in the DSCs. In Bode plots, the peak position of the middle frequency was related to the electron lifetime, a shift to lower frequency corresponded to a longer electron lifetime. The frequency in the peak position of the middle frequency of **T2** was lower than that of **T1**, so the order of the corresponding electron lifetime **T2** > **T1** was further in favour of the order of the V_{oc} of DSCs based on these two dyes.[22]

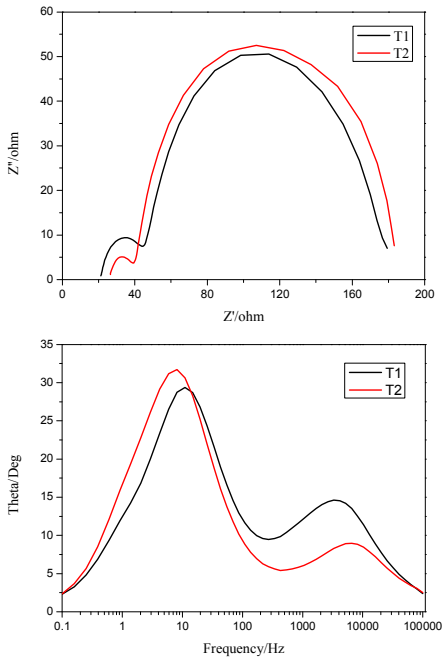

Fig. 6 Impedance spectra of DSCs based on **T1-T2** with dye baths of $CHCl_3$: EtOH (*v*/*v* 3:7) measured at a bias 0.70 V in the dark. (a) Nyquist plots; and (b) bode plots.

Conclusions

In summary, two new D-A-π-A dyes (**T1**-**T2**) with 5,7-dihexyl-6,12-diphenyl-5,7-dihydroindolo [2,3-b] carbazole as the donor, thiophene and phenyl as the linker, DPP and cyanoacrylic acid as the acceptor, were successfully synthesized. The results showed that the open circuit voltage (V_{oc}) could be improved by attaching the 2-ethyl-hexyl chain to the donor and the DPP unit, which proved to be an effective strategy to reduce the π-π aggregation of the dyes on TiO_2 films and suppress the charge recombination. Besides, short circuit photocurrent density (J_{sc}) was also enlarged by harvesting more photoelectrons on account of the effective conjugation of the donor would contribute to a high molar extinction coefficient. As a result, **T1** based-device achieved a higher overall conversion efficiency of 8.24% (J_{sc} of 15.72 mA cm^{-2}, V_{oc} of 0.739 V and *FF* of 0.71) in comparison with **T2** based-device that overall conversion efficiency of 7.83% (J_{sc} of 14.85 mA cm^{-2}, V_{oc} of 0.765 V and *FF* of 0.69). Furthermore, these results also indicated that the molecular engineering was important for fabricating highly efficient dyes in DSCs. A further study that the importance of bulky alkyl chains attached to the 5,7-dihexyl-6,12-diphenyl-5, 7-dihydroindolo [2,3-b] carbazole unit to opitimize the device performance and the measure to broaden the absorption spectra to the red/near-infrared region is in progress.

Experimental Section

Measurement and characterization

The ^1H and ^{13}C NMR spectra were recorded on a Brucker AM 400 spectrometer and Mass spectra were obtained on a Waters LCT Premier XE spectrometer. The UV-Vis absorption spectra of the dyes in solution and on dye-soaked films were measured with a Varian Cary 500 spectrophotometer. Elemental analyses were measured by German elementar vario EL III. The cyclic voltammograms of dyes were obtained from a Versastat II electrochemical workstation (Princeton applied research) with the conventional three electrode configuration as working electrode, a Pt wire counter electrode, and a regular calomel reference electrode in saturated KCl solution. The supporting electrolyte was 0.1M $TBAPF_6$ in CH_3CN. The scan rate was 100 mV s^{-1}. The potential of the reference electrode was calibrated by ferrocene and all the potential data in this paper were relative to normal hydrogen electrode (NHE). The electrochemical impedance spectroscopy (EIS) was measured with the DSCs being under dark using a Zahner IM6e Impedance Analyzer (ZAHNER-Elektrik GmbH & CoKG, Kronach, Germany). The spectra were scanned in a frequency range of 0.1-10^5 Hz with applied potential set at open circuit of the corresponding DSCs and the alternate current amplitude was set at 10 mV.

Materials

All reagents that we have used in the process were obtained from J&K Chemical Co. and Aladdin Chemical Co., which were received without further purification. Tetrahydrofuran (THF) and toluene were disposed by primary procedures.[8] The FTO conducting glass (F-doped SnO, transmission > 90% in the visible, sheet resistance 15Ω $square^{-1}$, Geao Science and Educational Co. Ltd. of China) was handled with detergent, redistilled water, ethanol, chloroform and acetone successively under supersonication for 30 min each before use. The DPP unit was prepared by the relevant procedures.[7]

Fabrication of DSCs

The thin TiO_2 films (12 μm) consisting of a transparent layer (Ti-Nanoxide T/SP) and a 4 μm scattering layer (Ti-Nanoxide 300) were coated on a well-cleaned FTO conducting glass using a screen printing technique, followed by calcinated at 500 ^oC under an air flow in muffle for 30 min.[23] When cooling down to the room temperature, the obtained films immersed in 0.05 M aqueous $TiCl_4$ solution for 30 min at 75 ^oC, after washed with redistilled water and anhydrous ethanol consecutively, then annealed at 450 ^oC for 30 min. After the obtained films being cool down and immersed into the dye solution (0.1 M in the required solvents) for 12 h, the dyes would load on the film. Then the working electrodes were rinsed with chloroform and anhydrous ethanol respectively. Deposited ~100 nm thick Pt on the conductive surface of the Pt-counter electrodes and drilled two holes (0.8-mm diameter) into the Pt-counter electrodes. A sandwich type solar cell was assembled with the working and Pt-counter electrodes and sealed with a hot-melt gasket of 25μm thickness. The electrolyte was injected into the cell from the holes and the fabrication of the solar cells was finally finished by sealing the holes using a UV-melt gum. The composition of the electrolytes was 0.1 M lithium iodide, 0.6 M 1,2-dimethyl-3-propylimidazolium iodide (DMPII), 0.05 M I_2, 0.5 M 4-tertbutylpyridine (4-TBP) in acetonitrile as a liquid electrolyte.

Synthesis:

3-(4-bromophenyl)-6-(4-(5,11-di(octan-3-yl)-6,12-diphenyl-5,11-dihydroindolo[3,2-b]carbazol-3-yl)phenyl)-2,5-di(octan-3-yl)pyrrolo[3,4-c]pyrrole-1,4(2H,5H)-dione (D-DDP) In a dry three-neck flask, adding 1.6 M n-BuLi in hexane (5 ml, 8.02 mmol, 15% solution) dropwise to the solution of compound **D-Br** (0.72 g, 1 mmol) in THF at -78 ^oC under a N_2 atmosphere. After stirring for 2 h at this temperature, triisopropyl borate (3.6 ml, 15.28 mmol, 98%) was added dropwise and put the mixture to r.t followed by stirring for 2 h. Then compound **DPP** (0.67 g, 1 mmol), K_2CO_3 (0.66 g, 4 mmol), $Pd(PPh_3)_4$ (30 mg, 0.03 mmol, 99.8%), water (4mL), and THF (12mL) were added and the mixture was heated to reflux after the flask was recharged with N_2. After refluxing for 6 h, the mixture cool down to r.t. and poured the mixture into water and extracted with CH_2Cl_2 (50 ml × 3). The organic layer was dried over anhydrous $MgSO_4$ and concentrated by using a rotary evaporator. The crude materials were purified by silica gel column chromatography (petroleum ether/CH_2Cl_2 = 4:1 V/V) to obtain a pale red solid 0.45 g, 39%. ^1H NMR (400 MHz, $CDCl_3$), δ: 7.86 (t, *J* = 7.8 Hz, 2H), 7.76 (t, *J* = 8.0 Hz, 2H), 7.65 (m, 4H), 7.62 – 7.58 (m, 10H), 7.53 (dd, *J* = 6.8, 3.0 Hz, 1H), 7.39 – 7.31 (m, 3H), 6.82 (m, 1H), 6.72 (s, 1H), 6.47 (t, *J* = 7.6 Hz, 1H), 3.97 – 3.93 (m, 4H), 3.89 – 3.81 (m, 4H), 1.50 – 1.46 (m, 8H), 1.35 (dd, *J* = 14.6, 7.4 Hz, 4H), 1.21 – 1.05 (m, 24H), 0.87 – 0.82 (m, 12H), 0.71 – 0.75 (m, 6H), 0.69 – 0.65 (m, 6H).

5-(4-(4-(4-(5,11-di(octan-3-yl)-6,12-diphenyl-5,11-dihydroindolo[3,2-b]carbazol-3-yl)phenyl)-2,5-di(octan-3-yl)-3,6-dioxo-2,3,5,6-tetrahydropyrrolo[3,4-c]pyrrol-1-yl)phenyl)thiophene-2-carbaldehyde (D-DDP-1) In a one-neck flash, compound **D-DPP** (2.07 g, 1.50 mmol), **D2** (0.52 g, 3.3 mmol, 97%), K_2CO_3 (0.83 g, 6 mmol), $Pd(PPh_3)_4$ (40 mg, 0.04 mmol, 99.8%), water (6 ml), and THF (18 ml) were added

and the mixture was heated to reflux for 4 h under N_2 atmosphere. After the mixture cool down to r.t. and poured the mixture into water and extracted with CH_2Cl_2 (100 ml × 3). The organic layer was dried over anhydrous $MgSO_4$ and concentrated by using a rotary evaporator. The crude materials were purified by silica gel column chromatography (petroleum ether/CH_2Cl_2 = 2:1 V/V) to obtain a red solid 1.52 g, 73%. ^{1}H NMR (400 MHz, $CDCl_3$), δ: 9.96 (s, 1H), 7.93 (t, *J* = 8.2 Hz, 2H), 7.87 (t, *J* = 8.0 Hz, 2H), 7.83 (m, 4H), 7.81 (t, *J* = 8.0 Hz, 2H), 7.75 (m, 2H), 7.70 – 7.67 (m, 8H), 7.52 (dd, *J* = 7.8, 4.0 Hz, 1H), 7.38 (t, *J* = 12.0 Hz, 1H), 7.34 (m, 2H), 6.85 (m, 1H), 6.72 (s, 1H), 6.45 (t, *J* = 7.8 Hz, 1H), 3.95 (t, *J* = 8.0 Hz, 2H), 3.90 (m, 2H), 3.88 – 3.84 (m, 4H), 1.52 – 1.47 (m, 8H), 1.35 (dd, *J* = 15.2, 7.8 Hz, 4H), 1.24 – 1.15 (m, 24H), 0.88 – 0.83 (m, 12H), 0.78 – 0.76 (m, 6H), 0.69 – 0.64 (m, 6H).

4'-(4-(4-(5,11-di(octan-3-yl)-6,12-diphenyl-5,11-dihydroindolo[3,2-b]carbazol-3-yl)phenyl)-2,5-di(octan-3-yl)-3,6-dioxo-2,3,5,6-tetrahydropyrrolo[3,4-c]pyrrol-1-yl)-[1,1'-biphenyl]-4-carbaldehyde(D-DPP-2) compound **D-DPP-2** was synthesized by the same procedure as described above for **D-DPP-1** using **D-DPP** and **D3** (98%). Yield: 76%. ^{1}H NMR (400 MHz, $CDCl_3$), δ: 10.12 (s, 1H), 8.03 (t, *J* = 7.8 Hz, 2H), 7.96 (t, *J* = 8.0 Hz, 2H), 7.85 (m, 6H), 7.78 (m, 1H), 7.69 – 7.63 (m, 10H), 7.53 (dd, *J* = 4.0, 8.0 Hz, 2H), 7.38 (t, *J* = 12.0 Hz, 1H), 7.33 (m, 2H), 6.83 (m, 1H), 6.71 (s, 1H), 6.46 (t, *J* = 7.6 Hz, 1H), 3.95 (t, *J* = 7.8 Hz, 2H), 3.91 (m, 2H), 3.88 – 3.83 (m, 4H), 1.33 – 1.26 (m, 12H), 1.18 – 1.12 (m, 18H), 1.02 – 0.98 (m, 6H), 0.89 (m, 6H), 0.81 – 0.76 (m, 12H), 0.69 – 0.64 (m, 6H).

(E)-2-cyano-3-(5-(4-(4-(4-(5,11-di(octan-3-yl)-6,12-diphenyl-5,11-dihydroindolo[3,2-b]carbazol-3-yl)phenyl)-2,5-di(octan-3-yl)-3,6-dioxo-2,3,5,6-tetrahydropyrrolo[3,4-c]pyrrol-1-yl)phenyl)thiophen-2-yl)acrylic acid(T1) In a one-neck flash, compound **D-DPP-1** (0.35 g, 0.3 mmol), 2-cyanoacetic acid (96 mg, 1.2 mmol, 95%) and three drops of piperidine in 20 ml THF was refluxed for 4 h under N_2 atmosphere. Upon cooling it, removed the mixture in vacuo. The residual was dissolved in 150 ml CH_2Cl_2 and extracted with water for three times. The combined organic layer was dried over anhydrous $MgSO_4$ and then concentrated by using a rotary evaporator. The crude materials were purified by silica gel column chromatography (methanol/CH_2Cl_2 = 1:1 V/V) to obtain a deep red solid 0.36 g, 86%. ^{1}H NMR (400 MHz, $CDCl_3$), δ: 7.87 (t, *J* = 8.0 Hz, 2H), 7.82 (s, 1H), 7.75 (m, 3H), 7.70 (t, *J* = 8.0 Hz, 1H), 7.68 (m, 2H), 7.66–7.63 (m, 10H), 7.51 (dd, *J* = 4.2, 8.0 Hz, 3H), 7.38 (t, *J* = 7.8, 4.0 Hz, 1H), 7.34 (m, 2H), 6.83 (m, 1H), 6.71 (s, 1H), 6.46 (t, *J* = 8.0 Hz, 1H), 3.95 (t, *J* = 8.0 Hz, 2H), 3.91 (m, 2H), 3.87 – 3.84 (m, 4H), 1.17 – 1.15 (m, 12H), 1.13 – 1.10 (m, 18H), 0.98 – 0.96 (m, 6H), 0.83 – 0.80 (m, 6H), 0.79 – 0.76 (m, 12H), 0.69 – 0.64 (m, 6H). ^{13}C NMR (126 MHz, THF – d_8), δ: 162.10, 161.92, 161.77, 145.91, 143.49, 143.12, 139.19, 138.88, 131.45, 129.73, 129.38, 128.98, 128.78, 125.01, 124.79, 123.11, 122.72, 122.24, 122.13, 118.24, 117.62, 117.45, 108.90, 105.25, 60.55, 56.81, 47.93, 39.38, 39.19, 38.09, 30.40, 30.36, 29.71, 29.62, 28.11, 22.96, 22.90, 22.80, 18.09, 13.41, 13.34, 9.89, 9.70, 9.63. HRMS (*m/z*): $[M - H]^+$ calcd for $C_{88}H_{96}N_5O_4S$, 1318.7183; found, 1318.7179. Anal. cald for $C_{88}H_{96}N_5O_4S$: C, 80.02; H, 7.40; N, 5.30. Found: C, 79.83; H, 7.29; N, 5.19%.

(E)-2-cyano-3-(4'-(4-(4-(5,11-di(octan-3-yl)-6,12-diphenyl-5,11-dihydroindolo[3,2-b]carbazol-3-yl)phenyl)-2,5-di(octan-3-yl)-3,6-dioxo-2,3,5,6-tetrahydropyrrolo[3,4-c]pyrrol-1-yl)-[1,1'-biphenyl]-4-yl)acrylic acid(T2) compound **T2** was synthesized by the same procedure as described above for **T1** using **D-DPP-2** and 2-cyanoacetic acid (95%). Yield: 89%. ^{1}H NMR (400 MHz, $CDCl_3$), δ: 8.02 (t, *J* = 8.0 Hz, 2H), 7.96 (t, *J* = 7.8 Hz, 2H), 7.82 (m, 6H), 7.69 (m, 1H), 7.68 – 7.66 (m, 10H), 7.51 (dd, *J* = 4.0, 8.0 Hz, 2H), 7.39 (t, *J* = 12.0 Hz, 1H), 7.35 (m, 2H), 6.83 (m, 1H), 6.71 (s, 1H), 6.46 (t, *J* = 7.8 Hz, 1H), 3.96 (t, *J* = 7.8 Hz, 2H), 3.91 (m, 2H), 3.88 – 3.85 (m, 4H), 1.28 – 1.26 (m, 12H), 0.98 – 0.91 (m, 18H), 0.82 – 0.80 (m, 6H), 0.79 (m, 6H), 0.67 – 0.69 (m, 12H), 0.66 – 0.64 (m, 6H). ^{13}C NMR (126 MHz, THF–d_8), δ: 162.79, 162.51, 162.19, 148.31, 143.94, 143.45, 139.26, 138.90, 131.53, 131.45, 129.53, 129.22, 129.09, 128.80, 128.06, 127.19, 126.76, 124.85, 122.73, 122.20, 118.29, 117.80, 117.53, 117.50, 108.97, 105.17, 58.93, 56.80, 48.00, 39.24, 39.21, 38.56, 30.34, 30.32, 29.76, 29.63, 28.17, 28.11, 28.07, 22.97, 22.85, 22.79, 18.08, 13.40, 13.35, 9.92, 9.87, 9.78. HRMS (*m/z*): $[M - H]^+$ calcd for $C_{90}H_{98}N_5O_4$, 1312.7619; found, 1312.7621. Anal. cald for $C_{90}H_{98}N_5O_4$: C, 82.22; H, 7.59; N, 5.33. Found: C, 82.20; H, 7.38; N, 5.15%.

Notes and references

[a] Key Laboratory for Advanced Materials and Institute of Fine Chemicals, East China University of Science & Technology, 130 Meilong Road, Shanghai, 200237, PR China. Fax: 862164252288. E-mail: bbsjh@ecust.edu.cn; huangjh@ecust.edu.cn.

[b] Division of Theoretical Chemistry and Biology, School of Biotechnology, KTH Royal Institute of Technology, SE-10691 Stockholm, Sweden.

†Electronic Supplementary Information (ESI) available: 1) The frontier orbital plots of the HOMO and LUMO of **T1-T2**; 2) Computational analysis; 3) absorption curves of dyes on TiO_2 films which were successively irradiated upon AM 1.5 solar light for 30 min; 4) Normalized absorption and emission spectra of **T1-T2** in both solvent systems; 5) the absorption amounts of **T1-T2** in $CHCl_3$: EtOH (*v*/*v* 3:7) and CH_2Cl_2; 6) The printout of elemental analysis of **T1-T2**.

1 (*a*) B. O'Regan and M. Grätzel, *Nature*, 1991, **353**, 737; (*b*) M. Grätzel, *Nature*, 2000, **35**, 3523; (*c*) M. K. Nazeeruddin, P. Péchy, T. Renouard, S. M. Zakeeruddin, R. Humphry-Baker, P. Comte, P. Liska, L. Cevey, E. Costa, V. Shklover, L. Spiccia, G. B. Deacon, C. A. Bignozzi and M. Grätzel, *J. Am. Chem. Soc.*, 2001, **123**, 1613; (*d*) H. Qin, S. Wenger, M. Xu, F. Gao, X. Jing, P. Wang, S. M. Zakeeruddin and M. Grätzel, *J. Am. Chem. Soc.*, 2008, **130**, 9202; (*e*) A. Mishra, M. K. R. Fischer and P. Bäuerle, *Angew. Chem., Int. Ed.*, 2009, **48**, 2474; (*f*) A. Hagfeldt, G. Boschloo, L. C. Sun, L. Kloo and H. Pettersson, *Chem. Rev.*, 2010, **110**, 6595.

2 (*a*) X. H. Zhang, Z. S. Wang, Y. Cui, N. Koumura, A. Furube and K. Hara, *J. Phys. Chem. C*, 2009, **113**, 13409; (*b*) H. N. Tian, Z. Yu, A. Hagfeldt, L. Kloo and L. C. Sun, *J. Am. Chem. Soc.*, 2011, **133**, 9413; (*c*) G. Calogero, G. D. Marco, S. Cazzanti, S. Caramori, R. Argazzi and C. A. Bignozzi, *Energy Environ. Sci.*, 2009, **2**, 1162; (*d*) X. Q. Meng, Y. Wang, M. L. Wang, J. L. Tu and F. M. Wua, *RSC Adv.*, 2013, **3**, 3304.

3 (*a*) N.-G. Park, *J. Phys. Chem. Lett*. 2013, **4**, 2423. (*b*) J.-H. Im, C.-R. Lee, J.-W. Lee, S.-W. Park, N.-G. Park, *Nanoscale*, 2011, **3**, 4088; (*c*) N. P., P. G., G. G., T.Y. Yang, M. K. N, J. Maier, and M. Grätzel, *Angew. Chem. Int. Ed*. 2014, **53**, 3151; (*d*) S. K, M. K. N, M. Grätzel, and S. Ahmad, *Angew. Chem. Int. Ed*. 2014, **53**, 2812.

4 (*a*) O. Enger, F. Nuesch, M. Fibbioli, L. Echegoyen, E. Pretsch and F. Diederich, *J. Mater. Chem.*, 2000, **10**, 2231; (*b*) H. Tian, X. C. Yang, R. K. Chen, Y. Z. Pan, L. Li, A. Hagfeldt and L. C. Sun, *Chem. Commun.*, 2007, **43**, 3741; (*c*) C. Teng, X. C. Yang, C. Yang, S. F. Li, M. Cheng, A. Hagfeldt and L. C. Sun, *J. Phys. Chem. C*, 2010, **114**, 9101; (*d*) G. D. Sharma, J. A. Mikroyannidis, M. S. Roy, K. R. J. Thomas, R. J. Balle and R. Kurchaniaf, *RSC Adv.*, 2012, **2**, 11457.

5 (*a*) A. Yello, H. W. Lee and M. Grätzel, *Science*, 2011, **344**, 629; (*b*) S. Qu and H. Tian, *Chem. Commun.*, 2012, **48**, 3039; (*c*) S. Y. Qu, C. J. Qin, A.Isam, Y. Z. Wu, W. H. Zhu, J. L. Hua, H. Tian, L.Y. Han, *Chem. Commun.*, 2012, **48**, 6972.

6 (*a*) B. Liu, W. H. Zhu, Q. Zhang, W. J. Wu, M. Xu, Z. J. Ning, Y. S. Xie and H. Tian, *Chem. Commun.*, 2009, **13**, 1766; (*b*) W. H. Zhu, Y. Z. Wu, S. T. Wang, W. Q. Li, X. Li, J. Chen, Z. S. Wang and H. Tian, *Adv. Funct. Mater.*, 2011, **21**, 756; (*c*) Y. Z. Wu and W. H. Zhu, *Chem. Soc. Rev.*, 2013, **42**, 2039; (*d*) X. H. Hu, S. Y. Cai, G. J. Tian, X. Li, J. H. Su, J. Li, *RSC Adv.*, 2013, **3**, 22544; (*e*) Y. Q. Wang, B. Chen, W. J. Wu, X. Li, W. H. Zhu, H. Tian, Y. S. Xie, *Angew. Chem. Int. Ed.*, 2014, **53**, 10779.

7 (*a*) J. C. Bijleveld, A. P. Zoombelt, S. G. J. Mathijssen, M. M. Wienk, M. Turbiez, D. M. Leeuw and R. A. J. Janssen, *J. Am. Chem. Soc.*, 2009, **131**, 16616; (*b*) W. Q. Li, Y. Z. Wu, X. Li, Y. S. Xie and W. H. Zhu, *Energy. Environ. Sci.*, 2011, **4**, 1830; (*c*) F. Zhang, K. J Jiang, J. H. Huang, C. C. Yu, S. G. Li, M. G. Chen, L. M. Yang, Y. L. Song, *J. Mater. Chem. A*, 2013, **1**, 4858.

8 (*a*) S. Y. Cai, G. J. Tian, X. Li, J. H. Su, H. Tian, *J. Mater. Chem. A*, 2013, **1**, 11295; (*b*) S. Y. Cai, X. H. Hu, G. J. Tian, H. T. Zhou, W. Chen, J. H. Huang, X. Li, J. H. Su, *Tetrahedron*, 2014, **70**, 8122.

9 (*a*) Y. Z. Wu, M. Marszalek, S. M. Zakeeruddin, Q. Zhang, H. Tian, M. Grätzel and W. H. Zhu, *Energy Environ. Sci.*, 2012, **5**, 8261; (*b*) S. Y. Cai, X. H. Hu, Z. Y. Zhang, J. H. Su, X. Li, A. Islam, L. Y. Han and H. Tian, *J. Mater. Chem. A*, 2013, **1**, 4763.

10 (*a*) P. Sonar, E. L. Williams, S. P. Singh and A. Dodabalapur, *J. Mater. Chem.*, 2011, **21**, 1053; (*b*) K. Do, D. Kim, N. Cho, S. Paek, K. Song and J. Ko, *Org. Lett.*, 2012, **14**, 222.

11 (*a*) N. Metri, X. Sallenave, C. Plesse, L. Beouch, P. –H. Aubert, F. Goubard, C. Chevrot and G. Sini, *J. Phys. Chem. C*, 2012, **116**, 3765; (*b*) X. B. Cheng, M. Liang, S. Y. Sun, Y. B. Shi, Z. J. Ma, Z. Sun and S. Xue, *Tetrahedron*, 2012, **68**, 5375.

12 (*a*) J. X. He, W. J. Wu, J. L. Hua, Y. H. Jiang, S. Y. Qu, J. Li, Y. T. Long and H. Tian, *J. Mater. Chem.*, 2011, **21**, 6054; (*b*) J. Y. Mao, F. L. Guo, W. J. Ying, W. J. Wu, J. Li and J. L. Hua, *Chem.–Asian J.*, 2012, **7**, 982; (*c*) B. Liu, W. H. Zhu, Y.Q. Wang, W. J. Wu, X. Li, B. Q. Chen, Y. T. Long, Y. S. Xie, *J. Mater. Chem.*, 2012, **22**, 7434; (*d*) Y. Q. Wang, X. Li, B. Liu, W. J. Wu, W. H. Zhu, Y. S. Xie, *RSC Adv.*, 2013, **3**, 14780.

13 (*a*) R. Katoh, A. Furube, S. Mori, M. Miyashita, K. Sunahara, N. Koumura and K. Hara, *Energy Environ. Sci.*, 2009, **2**, 542; (*b*) M. Chen, X. C. Yang, J. H. Zhao, C. Chen, Q. Tan, F. G. Zhang and L. C. Sun, *ChemSusChem*, 2013, **6**, 2322.

14 Becke, A. D. *J. Chem. Phys*. 1993, **98**, 5648.

15 Hehre, W. J.; Ditchfield, R.; Pople, J. A. *J. Chem. Phys*. 1972, **56**, 2257.

16 Yanai, T.; Tew, D. P.; Handy, N. C. *Chem. Phys. Lett.* 2004, **393**, 51.

17 Schäfer, A.; Huber, C.; Ahlrichs; R. *J. Chem. Phys*. 1994, **100**, 5829.

18 Frisch, M. J.; Trucks, G. W.; Schlegel, H. B.; Scuseria, G. E.; Robb, M. A.; Cheeseman, J. R.; Scalmani, G.; Barone, V.; Mennucci, B.; Petersson, G. A.; et al. Gaussian 09, revision A.2; Gaussian, Inc.: Wallingford CT, 2009.

19 (*a*) S. Hwang, J. H. Lee, C. Park, H. Lee, C. Kim, C. Park, M. H. Lee, W. Lee, J. Park, K. Kim, N. G. Park and C. Kim., *Chem. Commun.*, 2007, **46**, 4887; (*b*) C. -J. Yang, Y. J. Chang, M. Watanabe, Y. -S. Hon, T. J. Chow. *J. Mater. Chem*., 2012, **22**, 4040.

20 (*a*) J. Tang, W. J. Wu, J. L. Hua, X. Li and H. Tian, *Energy. Environ. Sci.*, 2009, **2**, 982; (*b*) L. Wang, H. Y. Wang, H. H. Fang, H. Wang, Z. Y. Yang, B. R. Gao, Q. D. Chen, W. Han and H. B. Sun, *Adv. Funct. Mater.,* 2012, **22**, 2783; (*c*) H. H. Chou, Y. C. Chen, H. J. Huang, T. H. Lee, J. T. Lin, C. Tsai and K. Chen, *J. Mater. Chem*., 2012, **22**, 10929.

21 (*a*) A. Morandeira, I. López-Duarte, B. O'Regan, M. V. Martínez-Díaz, A. Forneli, E. Palomares, T. Torres and J. R. Durrant, *J. Mater. Chem.*, 2009, **19**, 5016; (*b*) H. Ozawa, M. Awa, J. Ono, and H. Arakawa. *Chem.–Asian J*., 2012, **7**, 156; (*c*) Y. Cui, Y. Z. Wu, X. F. Lu, X. Zhang, G. Zhou, F. B. Miapeh, W. H. Zhu and Z. S. Wang, *Chem. Mater.*, 2011, **23**, 4394.

22 (*a*) R. Katoh, A. Furube, S. Mori, M. Miyashita, K. Sunahara, N. Koumura and K. Hara, *Energy Environ. Sci.*, 2009, **2**, 542; (*b*) C. Y. Wang, J. Li, S. Y. Cai, Z. J. Ning, D. M. Zhao, Q. Zhang and J. H. Su, *Dyes and Pigments*, 2012, **94**, 40; (*c*) C. Chen, X. C. Yang, J. J. Li, F. G. Zhang and L. C. Sun, *ChemSusChem*, 2013, **6**, 70.

23 A. Schaefer, H. Horn and R. Ahlrichs, *J. Chem. Phys*., 1992, **97**, 2571.